Sarcouncil Journal of Applied Sciences

ISSN(Online): 2945-3437

Volume- 05| Issue- 09| 2025

Research Article **Received:** 30-07-2025 | **Accepted:** 20-08-2025 | **Published:** 16-09-2025

Effect of Jumping Energy Coefficient on Armchair-Type Graphene Energy Gap

H. Z. Bashar

Department of Physics, College of Science, AL-Muthanna University, AL-Muthanna, IRAQ

Abstract: This work examines the electronic band structure of bilayer armchair-type graphene nanoribbons arranged in the AB stacking pattern. The investigation is conducted using the long-wave generalised effective Hamiltonian and the tight approximation method. This investigation involved calculating the energy gap values for various electron hopping energy levels between two layers. Additionally, the widths were varied from N = 1 to N = 10, with increments of 5 until reaching N = 50. An evident correlation was detected between the electron hopping energies and the energy gap and width of the nanoribbon. Specifically, as the electron hopping energy dropped, both the energy gap and the breadth of the nanoribbon increased. The nanoscale had a non-uniform impact on the energy gap values, unlike the abrupt change in energy caused by certain boundary conditions when solving the Schrödinger equation around the Dirac points K in the Fermi plane. At certain values, the material exhibits metallic behaviour, while at others it acts as a semiconductor. Hence, this study provides valuable insights into the properties of graphene. Theoretical confirmation suggests that the energy gap can be manipulated by adjusting the hopping energies of electrons between two layers of armchair-type graphene nanoribbons with a specific stacking pattern (AB-AB). Additionally, the width of the nanoribbon also influences this effect.

Keywords: Multilayers Armchair Graphene Nanoribbon (MLAGNRs), Band Structure, Energy Gap, Tight Binding Approximation.

INTRODUCTION

Graphene, discovered in 2004 by Andre Geim and Konstantin Novoselov, has attracted scientific interest due to its remarkable features (Wasalathilake, K. C. *et al.*, 2020). It is regarded as a semiconductor material with a zero-energy gap. The magnitude of this energy gap may be manipulated by several elements, mostly through engineering techniques, without necessitating alterations to the crystal structure of graphene, as is often done with conventional semiconductors (Potbhare, A. K. *et al.*, 2024). Due to its significant property and the scientific advancements in miniaturising electronic devices, several researchers were motivated to investigate the electronic characteristics of graphene. This research article falls within the scope of this research area (Gosling, J. H. *et al.*, 2021; Gosling, J. H. *et al.*, 2021). Graphene is classified as a two-dimensional (2D) substance (Kotov, V. N. *et al.*, 2012). The carbon atoms are organised in a hexagonal lattice structure like a honeycomb (Di Bernardo, I. *et al.*, 2018). Due to carbon's tetravalent nature, it is capable of forming two distinct forms of covalent bonds (Gosling, J. H. *et al.*, 2021). The strong form of bond between carbon atoms in the honeycomb structure is known as (δ). The other is feeble, referred to as (π)(Neto, C. *et al.*, 2009). The bonds in the graphene lattice are formed by SP^2 hybridisation (Barlocco, I. *et al.*, 2020). The final bond is accountable for the entirety of the electronic, electrical, thermal, and magnetic characteristics. The mechanical characteristics are determined by the bond (δ)(Novoselov, K. S. *et al.*, 2007). The majority of graphene's characteristics, including as its exceptional electrical and thermal conductivity, as well as its electronic properties, manifest mostly near its edges (Balandin, A. A. 2011; *materials* 10.8 (2011): 569-581.

Renteria, J. D. *et al.*, 2014). Hence, graphene edges are categorised into two primary types: a zigzag-shaped edge and another referred to as an armchair (Enoki, T. *et al.*, 2012). Additionally, there exists a third category that is a blend of the two primary categories. The crystal structure of the graphene lattice consists of two sub lattices, known as the A and B lattices, which are not equal in size (Yang, G. *et al.*, 2018). The π bond in the electronic structure of the lattice is in close proximity to the Fermi level, and its electrons exhibit the characteristics of massless fermions (Zhan, D. *et al.*, 2012). The valence and conduction bands of this crystal structure intersect at the unequal Dirac points, known as ($K+$, $K-$), which form two opposed cone shapes (Wakabayashi, K. *et al.*, 2010). Recently, there has been a focus on researching graphene nanoribbons, which may be classified into two categories based on their edge structure. The initial category is referred to as zigzag, whereas the subsequent one is denoted as armchair (Liu, J., & Feng, X. 2020). The first kind is distinguished by a pronounced edge effect in close proximity to the Dirac points, resulting in the nanoribbon exhibiting metallic behaviour. Regarding the second kind, it has the potential to be It exhibits metallic or semiconductor properties based on specific boundary conditions at the Dirac points, which are

***Corresponding Author:** H. Z. Bashar

DOI- https://doi.org/10.5281/zenodo.17132494

defined by the equation $n = 3p + 2$. The armchair-type graphene nanoribbon exhibits metallic behaviour, whereas the condition ($n = 3p$ or $n = 3p + 1$) indicates semiconductor properties (Wakabayashi, K. *et al.*, 2009; Sun, Q. *et al.*, 2020). If the core tape consists of a single layer, these two criteria are applicable. However, when the core tape is composed of double or triple layers, the presence of multiple layers disrupts these two conditions. Here, p represents an integer and n denotes the number of atom locations on the edge of the nanoribbon (Majid, M. J., & Alaa, M. H. 2018). When it comes to multilayer graphene, whether it is in the form of flat sheets or nanoribbons, there are two fundamental ways in which it can be stacked: either in an ABC-ABC pattern or an AB-AB pattern (Lavor, I. R. *et al.*, 2020). Van der Waals forces mediate the interaction between many layers of graphene and have a limited impact on its electrical characteristics due to the treatment of the π electrons linked to the weak bond as particles. Massless particles, also known as free-moving particles, are governed by the Dirac equation for free electrons (Lee, J. H. *et al.*, 2015). The electric characteristics of graphene nanoribbons exhibit variability based on several parameters, such as the specific stacking arrangement. This research study will utilise AB stacking and a bilayer configuration. The electrical characteristics of these nanoribbons are determined by two additional factors: the width of the nanoribbons and the hopping energy, which refers to the ability of an electron to move between the two layers (Richter, N. *et al.*, 2020). This energy influences the difference in energy levels between the two layers. Graphene nanoparticles exhibiting semiconductor behaviour. The hopping energy may be computed using a tight binding approximation (Behura, S. K. *et al.*, 2019).

Computation Details

Graphene nanoribbons may be categorised into two fundamental types: armchairs and zigzags, as previously noted. Furthermore, apart from the aforementioned distinction, there exists a significant disparity between them that compels us to examine the first category. Firstly, there is an estimated discrepancy of 30 in the edge angle (Zhang, J. *et al.*, 2019; Kim, J., Lee. *Et al.*, 2018). The second form, zigzags, exhibits localised energy states while the first type does not. The armchair represents different energy levels, and as a result, the energy band structures may be represented visually based on the transverse wavenumber. We can consider the transverse wavenumber as quantised values in momentum space. Regarding the second type, it is not possible to do so because the wavenumber of the longitudinal wave is influenced by both the wavenumber of the transverse wave and the width of the nanoribbon. Therefore, we have selected Armchair type graphene. tapes to analyse the energy band structures, which can be utilised in the production of graphene-based electronic chips (Lavor, I. R. *et al.*, 2020).

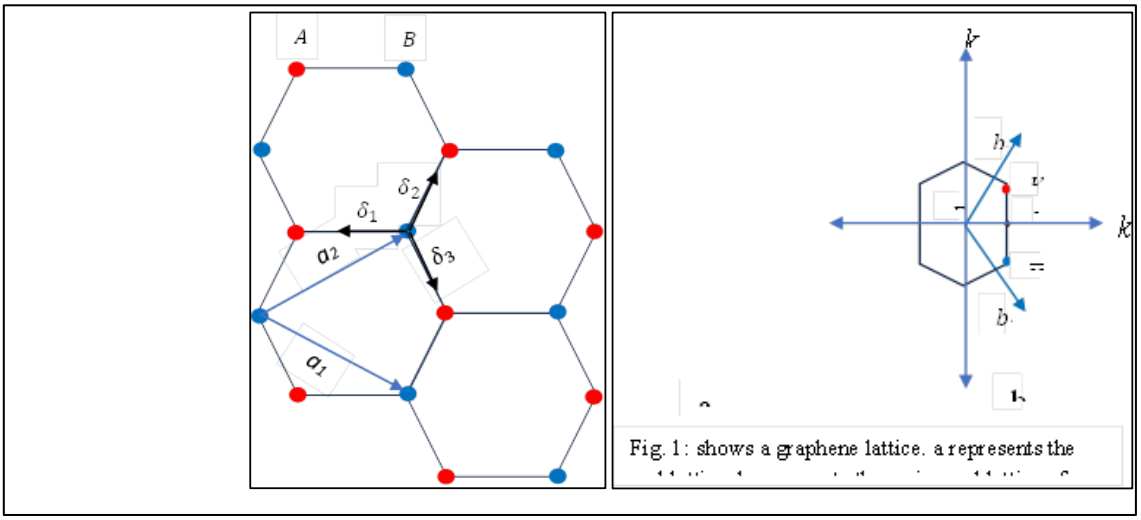

Fig:1 shows a grapheme a represents the

Figure 1 depicts the actual and mirrored hexagonal lattice structure of graphene. It is widely recognised that the hexagonal lattice does not conform to the characteristics of a paravisian lattice. Hence, the hexagonal lattice is partitioned into two triangular paravisian lattices (Thomson, A. *et al.*, 2018), shown by the red and blue dots in Figure (1a). The fundamental transition vectors of

Publisher: SARC Publisher

the paravisian lattice, denoted as a_1 and a_2, are expressed as:

$a_1 = \frac{a}{2}(3, \sqrt{3})$, $a_2 = \frac{a}{2}(3, -\sqrt{3})$

The variable a denotes the distance between two carbon atoms in the paravisc lattice, with an estimated value of a=0.142 nm. (Molitor, F. *et al.*, 2011) In regards to the reverse lattice of graphene, seen in Figure (1b), the vectors b_1 and $b_2$may be expressed as follows:

$b_1 = \frac{2\pi}{3a}(1, \sqrt{3})$, $b_2 = \frac{2\pi}{3a}(1, -\sqrt{3})$

2

Fig (1b) displays two crucial sites that significantly influence the electrical characteristics of graphene sheets and nanoribbons. The entities in question are K and $\overline{K}$. The two points are referred to as Dirac points, and their locations in momentum space are determined using the following equations.

$K = \frac{2\pi}{3a}\left(1, \frac{1}{\sqrt{3}}\right)$, $\overline{K} = \frac{2\pi}{3a}\left(1, -\frac{1}{\sqrt{3}}\right)$

3

The vectors $(\delta_1, \delta_2, \delta_3)$ in real space correspond to the three closest neighbours, and their positional equations are expressed in the following forma (Neto, C. *et al.*, 2009):

$\delta_1 = \frac{a}{2}(1, \sqrt{3})$, $\delta_2 = \frac{a}{2}(1, -\sqrt{3})$, $\delta_3 = -a(1,0)$

4

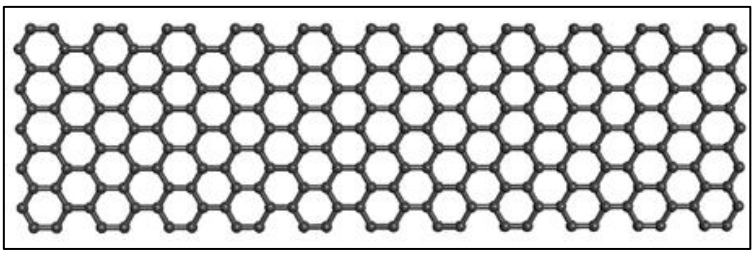

Fig. 2: The diagram indicates a graphene nanoribbon of length *L* and width *W* respectively with armchair edges (AGNR).

In Figure 2, the width of the armchair type graphene nanoribbon is calculated by counting the number of carbon atom positions in the unit cell in the y direction, according to the given relationship.

$W = \frac{N}{4} a_o \sqrt{3}$

5

The variable a_o denotes the lattice constant of graphene, whereas N indicates the number of carbon atom locations in the unit cell along the width of the nanoribbon. The energy of the armchair graphene nanoribbon may be determined using the tight-binding approximation, which relies on the nearest-neighbor connection (Molitor, F. et al., 2011).

$E(k, k_q) = S v_F \hbar \mathcal{E}$

6

$\mathcal{E} = \sqrt{1 + 4\cos(k_q)\cos\left(\frac{k}{2}\right) + 4\left(\cos(k_q)\right)^2}$

7

Relation 6 describes the energy in momentum space, specifically in terms of the wave vector k. In this context, k_q represents the quantised values of the transverse wave vector. The symbol $v_F$represents the Fermi velocity of electrons on the surface of the graphene nanoribbon, which is approximately 300 times smaller than the velocity of light in a vacuum (10^6 m/sec)(Tene, T. *et al.*, 2022). Lastly, k represents the longitudinal wave vector for the wave packet. The boundary conditions of the armchair graphene nanoribbon (AGNR) for the transverse component of the $k_q$wave vector allowed us to determine the quantised values of k_q and the subsequent results:

$k_q = \frac{2}{a\sqrt{3}} \frac{q}{N+1}$, $q = 1,2,3, \ldots, N$

8

The bond length of the graphene sheet lattice is represented by a and q is an integer (Lavor, I. R. *et al.*, 2020) The Hamiltonian that accurately describes the behaviour of graphene nanoribbons in the first Brillouin zone, namely at the K point of AB stacking, may be mathematically represented as follows:

$$H_n = \hbar v_F \begin{pmatrix} \sigma.k & \tau \cdots & 0 \\ \tau^+ & \sigma.k \ldots & 0 \\ 0 & \tau^+ & \sigma.k \end{pmatrix}$$

9

Where τ represent the 2×2 coupling matrix as follows:

$$\tau = \frac{1}{\hbar v_F} \begin{pmatrix} 0 & \gamma_i \\ 0 & 0 \end{pmatrix}$$

10

The symbol $\gamma_i$denotes the energies associated with electron movement between the two layers of graphene nanoribbon in AB stacking (Lavor, I. R. *et al.*, 2020). These energies may be determined using the following general equation:

$\gamma_i = \int \varphi_m^*(r - r_m) H \varphi_n(r - r_m \pm R_{mn}^j \pm \mu h)$

11

Publisher: SARC Publisher

$m, n = A$ *or* B , $= 1,2,3$, $\mu = 0$ *or* 1 *Where A and B refer to the graphene sublattice, h represents* the distance between the layers of graphene, which is approximately equal to $h = 0.335\text{nm}$. $R_{AB}^{1} = a\left(\frac{1}{\sqrt{3}}, 0, 0\right)$, $R_{AB}^{2} = a\left(\frac{-1}{2\sqrt{3}}, \frac{1}{2}, 0\right)$, $R_{AB}^{3} = a\left(\frac{-1}{2\sqrt{3}}, \frac{-1}{2}, 0\right)$. R_{AB}^{j}denotes the spatial coordinates of the atoms within the binary graphene lattice. For this study, we selected three specific numbers to represent the electron hopping energy in a graphene nanoribbon consisting of two layers arranged in the AB stacking manner. These values are(Partoens, B., & Peeters, F. M. 2006; Chung, D. D. L. 2002)

- $\gamma_1 = 0.377\text{eV}$ $A_1 \rightarrow B_2$
- $\gamma_3 = 0.290\text{eV}$ $B_1 \rightarrow B_2$
- $\gamma_4 = 0.120\text{eV}$ $A_1 \rightarrow A_2$
- Figure 3 depicts two layers of graphene arranged in AB stacking, with the corresponding values denoted as γ_i.

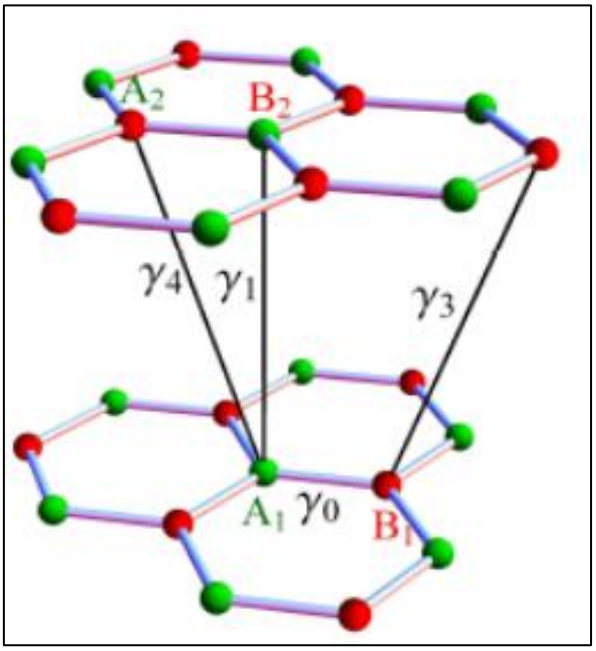

Fig. 3: Schematic diagram of AB-stacked bilayer graphene with electron hopping energies shown $\gamma_1, \gamma_3, \gamma_4$ (Konschuh, S. *et al.*, 2012)

The monolayer graphene Hamiltonian is directly represented by the diagonal in Equation (9). At low energy levels, about. The generalised Hamiltonian may be restated in the following manner:

$$H_n(k) = \frac{(\hbar v_F k)^n}{\gamma^{n-1}} \begin{pmatrix} 0 & e^{-in\phi} \\ e^{in\phi} & 0 \end{pmatrix}$$

12

The symbol ϕ denotes the polar angle in a two-dimensional momentum space, whereas n represents the number of layers. The physical boundary conditions at the borders of the armchair graphene nanoribbon are as follows:

$$\psi_A(x = 0) = \psi_B(x = 0) = \psi_A(x = L) = \psi_B(x = L) = 0$$

13

Here is the spinor wave function of the Hamiltonian:

$$\psi(r) = e^{ik_y y} \begin{pmatrix} \phi_A(x) \\ \phi_B(x) \end{pmatrix}$$

14

The below text is an approximate representation of the generalised formula for the energy spectrum of an n-layer (AB) stacking armchair graphene nanoribbon (Majid, M. J., & Alaa, M. H. 2018).

$$E_n = S\hbar v_F \sqrt{1 + 4\cos(k_q^n)\cos\left(\frac{k^n}{2}\right) + 4\frac{[\cos(k_q^n)]^2}{\gamma^{n-1}}}$$

15

where $S = \pm 1$ *(*$S = +1$ *and* $S = -1$ *stand for the valence and conduction energy bands, respectively. The transversal wave number* k_n *is given by:*

$$k_q = \frac{m\pi}{N+1} \quad , \quad m = 1,2,3,4, \ldots, N$$

16

This approximation becomes more important as the number of layers (n) grows and is only valid for the low-energy range of energy. The direct energy gap of Armchair graphene nanoribbons is always seen at the k = 0 point.

DISPLAY RESULTS

This section examines the electronic structure ranges of an armchair-type graphene nanoribbon

Publisher: SARC Publisher

with AB stacking. The analysis focusses on the width of the ribbon and the hopping energy of electrons between two layers of the graphene nanoribbon. Three specific values of the hopping energy ($\gamma = 0.377, 0.290, 0.120$ eV) are considered. The width of the ribbon ranges from N=1 to N=10, with a regular increase in the number of atoms. First, start with N=10 and increase it by five atoms until N=50. By using equations 15 and 16. The forces between the layers are van der Waals forces, which are known to be minimal. Although these forces were initially disregarded in the computations, their impact indirectly manifests through the levels of electron hopping between the two layers, denoted as γ. We will analyse the impact of both the nanoribbon's width and the hopping energy of the electrons between the two layers on the electrical structure bands. We will examine the impact of these two variables on the energy gap values of this specific type of graphene nanoribbons and this particular stacking technique.

Table 1. shows the energy gap values for different values of electron hopping energies between two layers of armchair type graphene nanoribbon for different values of width in terms of N.

$\gamma = 0.12\ eV$		$\gamma = 0.29\ eV$	$\gamma = 0.377\ eV$
N	E_g	E_g	E_g
1	*0.68984*	*0.38788*	*0.29836*
2	*0.14704*	*0.06084*	*0.04680*
3	*0.81454*	*0.33704*	*0.25926*
4	*1.38846*	*0.58376*	*0.44906*
5	*0.14704*	*0.06084*	*0.04680*
6	*0.22522*	*0.09320*	*0.06154*
7	*0.68968*	*0.28538*	*0.04384*
8	*0.14704*	*0.06084*	*0.01792*
9	*0.43698*	*0.18082*	*0.02760*
10	*0.05308*	*0.02196*	*0.01690*
15	*0.23646*	*0.04892*	*0.07526*
20	*0.14704*	*0.06084*	*0.04680*
25	*0.09158*	*0.03790*	*0.00734*
30	*0.06440*	*0.02664*	*0.02050*
35	*0.0443*	*0.01832*	*0.0141*
40	*0.07202*	*0.02980*	*0.02292*
45	*0.02622*	*0.01084*	*0.00874*
50	*0.01316*	*0.00544*	*0.00544*

Table 1 displays the energy gap values for three electron hopping energy levels and several width values. We have made many observations. Typically, the impact of the hopping energy is evident in the energy gap values, which exhibit an inverse relationship with the electron hopping energy. This means that as the hopping energy decreases, the energy gap grows. This connection holds true for a given nanoribbon width. This alteration is not comprehensible from a physical perspective. Indeed, the clarity of the situation is evident in the context of equations, namely Equation 15. However, from a physical standpoint, the rationale for this phenomenon may be attributed to the well-established fact that graphene is classified as a semiconductor material with a zero-energy gap, thereby exhibiting metallic behaviour. In order to create an energy gap without any external factors, we can modify the geometric dimensions of a single layer or increase the number of layers. In this context, the electron hopping energy has a subordinate significance. As previously mentioned, the hopping energy varies depending on the type of transition. Due to the nearly constant electron energy inside a single layer, the electron depletes its energy when transitioning between graphene layers. Consequently, when the hopping energy is low, the electron preserves a greater amount of energy compared to when the hopping energy is high, enabling it to occupy higher energy levels. The energy gap represents the disparity in energy levels between the conductivity and valence bands. Consequently, when the jump energy is minimal and the nanoribbon width remains constant, the energy gap values tend to be significant. The clarity of the information may be observed by examining Figures 4, 5, 6, 7, and 8, which depict a collective total of 54 Figures illustrating energy and k in momentum space. Figure 3 displays the

Publisher: SARC Publisher

energy spectrum of a graphene nanoribbon with an armchair shape and a width of N=3. The graph illustrates the impact of different electron hopping energies on the energy gap.

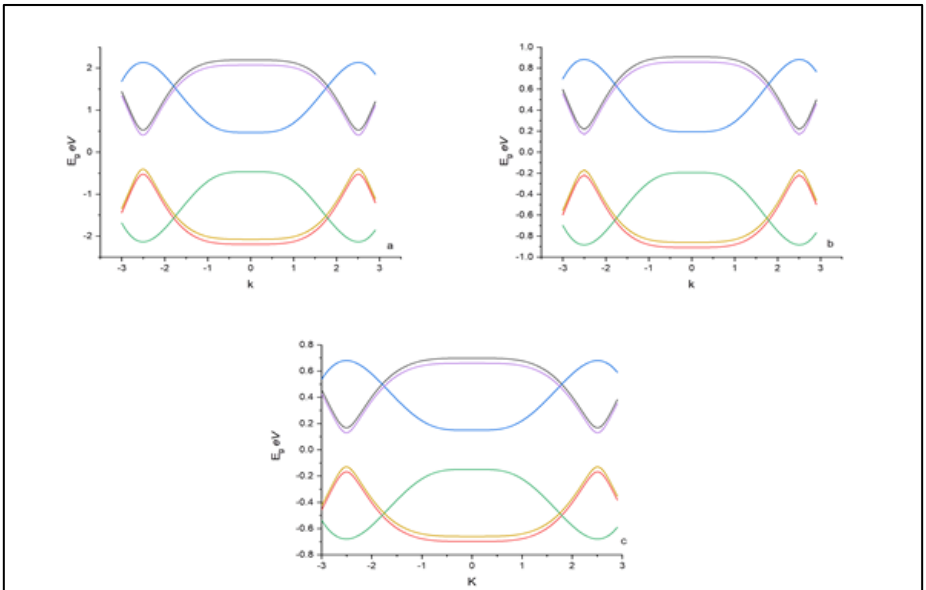

Fig.4. Energy spectrum of N=3 bilayer armchair graphene nanoribbon for different electron hopping energy values: (a) $\gamma_1 = 0.12$, (b) $\gamma_2 = 0.0.29$ (c) $\gamma_3 = 0.377$.

Fig.4. Energy spectrum of N=3 bilayer armchair graphene nanoribbon for different electron hopping energy values: (a) $\gamma_1 = 0.12$, (b) $\gamma_2 = 0.0.29$ (c) $\gamma_3 = 0.377$.

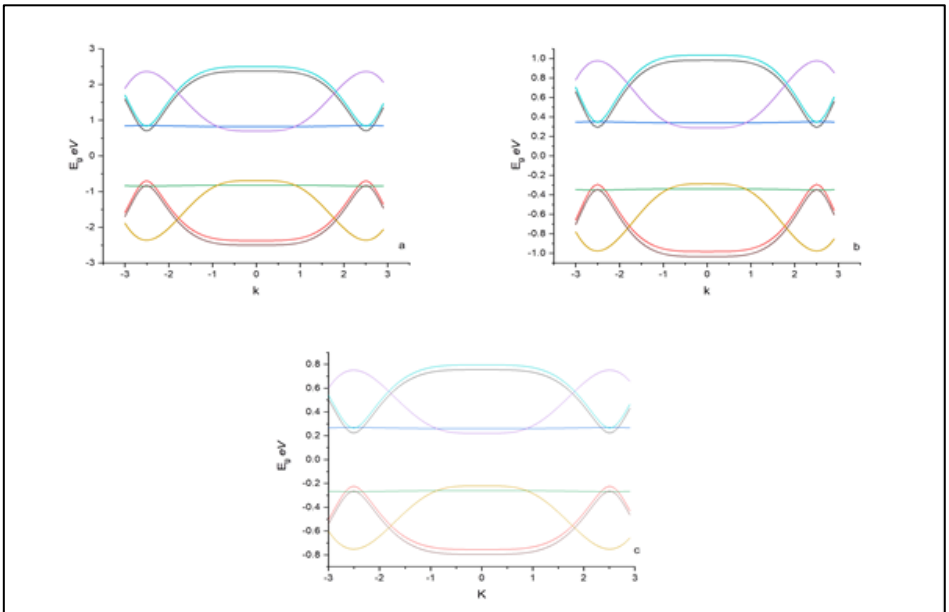

Fig.5. Energy spectrum of N=4 bilayer armchair graphene nanoribbon for different electron hopping energy values: (a) $\gamma_1 = 0.12$, (b) $\gamma_2 = 0.0.29$ (c) $\gamma_3 = 0.377$.

Fig. 5: Energy spectrum of N=4 bilayer armchair graphene nanoribbon for different electron hopping energy values: (a) $\gamma_1 = 0.12$, (b) $\gamma_2 = 0.0.29$ (c) $\gamma_3 = 0.377$.

Figure 5 displays the energy spectrum of a graphene nanoribbon with an armchair shape and a width of N=4. The spectrum is shown for three different values of electron hopping energy. The impact of the hopping energy on the energy gap is evident, and our calculations indicate that the optimal value is γ=0.12eV. Additionally, when compared to the other figures, the best result is achieved with a width of N=4.

Publisher: SARC Publisher

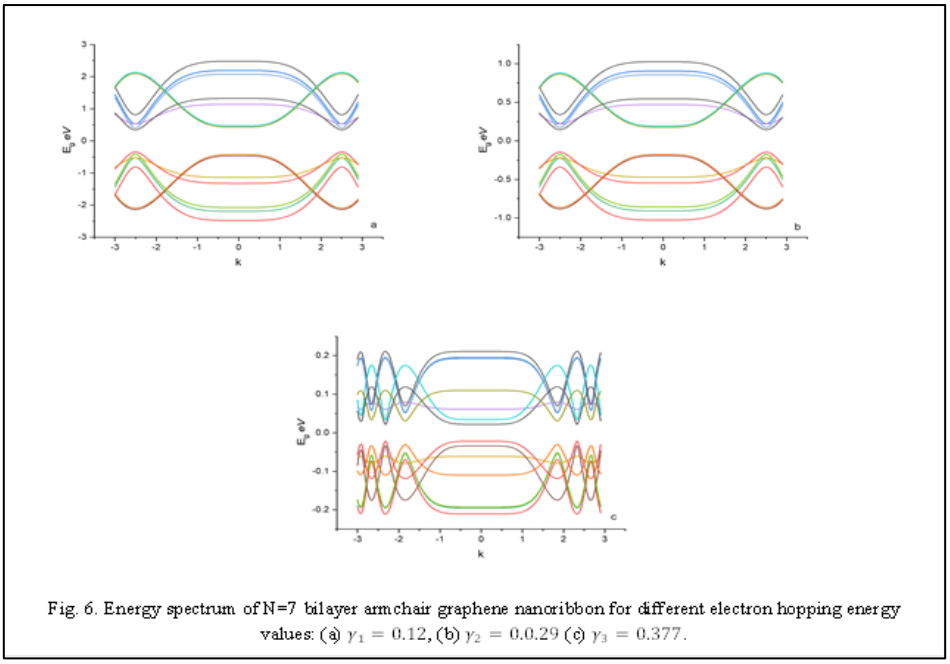

Fig. 6. Energy spectrum of N=7 bilayer armchair graphene nanoribbon for different electron hopping energy values: (a) $\gamma_1 = 0.12$, (b) $\gamma_2 = 0.0.29$ (c) $\gamma_3 = 0.377$.

Fig. 6: Energy spectrum of N=7 bilayer armchair graphene nanoribbon for different electron hopping energy values: (a) $\gamma_1 = 0.12$, (b) $\gamma_2 = 0.0.29$ (c) $\gamma_3 = 0.377$.

Figures 6, 7, and 8 depict the width in relation to N values of 7, 9, and 15. By comparing these figures with the energy gap values from Table 1, we observe that the arrangement of energy gap values, when γ is set to 0.12, follows a descending order from highest to lowest for N values of 7 and 9, and then 15. However, when the value of γ is 0.29, we observe that the energy gap value at N = 15 is lower than the previous arrangement, as well as for $\gamma = 0.377$. Therefore, we are unable to identify a consistent pattern that determines the energy gap values when the nucleus band width and electron hopping energy values vary. The maximum energy gap value among the three cases always occurs at N = 4, with the optimal value being $\gamma = 0.12$. At this point, the energy gap (Eg) is equal to 1.38846, which is comparable to traditional semiconductors like silicon and germanium (Eg = 1.08, 0.65eV) as individual elements (Herman, F. 2007), as well as compounds like indium phosphide (InP) (Eg = 1.42eV) and gallium arsenide (Eg = 1.43eV). Regarding traditional semiconductors (Gayen, R. N. *et al.*, 2012).

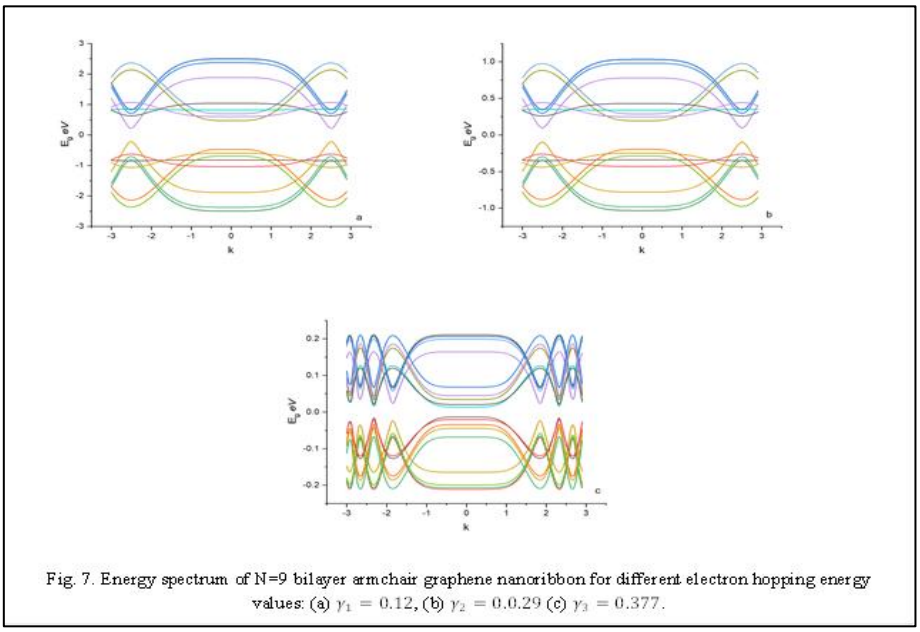

Fig. 7. Energy spectrum of N=9 bilayer armchair graphene nanoribbon for different electron hopping energy values: (a) $\gamma_1 = 0.12$, (b) $\gamma_2 = 0.0.29$ (c) $\gamma_3 = 0.377$.

Fig. 7: Energy spectrum of N=9 bilayer armchair graphene nanoribbon for different electron hopping energy values: (a) $\gamma_1 = 0.12$, (b) $\gamma_2 = 0.0.29$ (c) $\gamma_3 = 0.377$.

Publisher: SARC Publisher

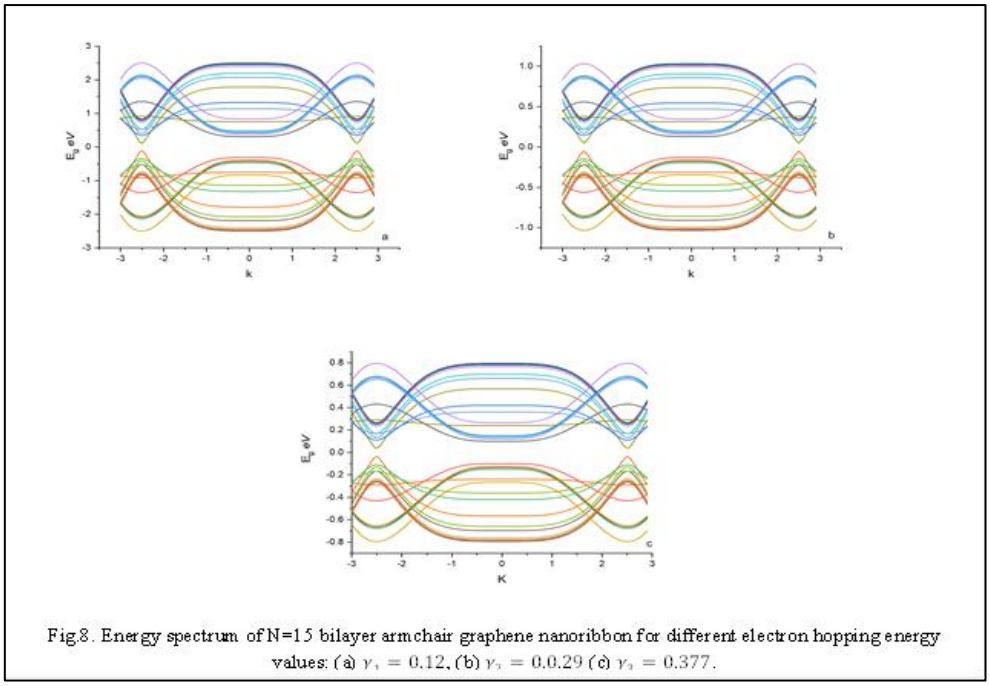

Fig.8. Energy spectrum of N=15 bilayer armchair graphene nanoribbon for different electron hopping energy values: (a) $\gamma_1 = 0.12$, (b) $\gamma_2 = 0.0.29$ (c) $\gamma_3 = 0.377$.

Fig. 8: Energy spectrum of N=15 bilayer armchair graphene nanoribbon for different electron hopping energy values: (a) $\gamma_1 = 0.12$, (b) $\gamma_2 = 0.0.29$ (c) $\gamma_3 = 0.377$.

Figure 9 illustrates the correlation between the width of the armchair graphene nanoribbon and the energy gap values for three different electron hopping energy values. There is a noticeable resemblance in the trend of energy gap values changing with width for the values $\gamma = 0.12$ and 0.29, in contrast to when $\gamma = 0.377$. The explanation for this may be attributed to the proximity of the two numbers, since the discrepancy between them is around 0.17, but the discrepancy between $\gamma = 0.377$ and $\gamma = 0.12$ is nearly 0.25. Additionally, we see a distinct anomaly in the fluctuations of the energy gap values, particularly at lower width values. However, a pattern starts to emerge as the width value reaches N = 10 for all three forms a, b, and c. It can be inferred that when the width of the armchair graphene nanoribbon is within the range of N=1 to N=9 and the electron hopping energy between two layers of graphene is low, the regular pattern in the energy gap change with the width of the nanoribbon is lost. The regular pattern in the energy gap values only starts to emerge when the width increases, particularly when the width of the nanoribbon is N>10.

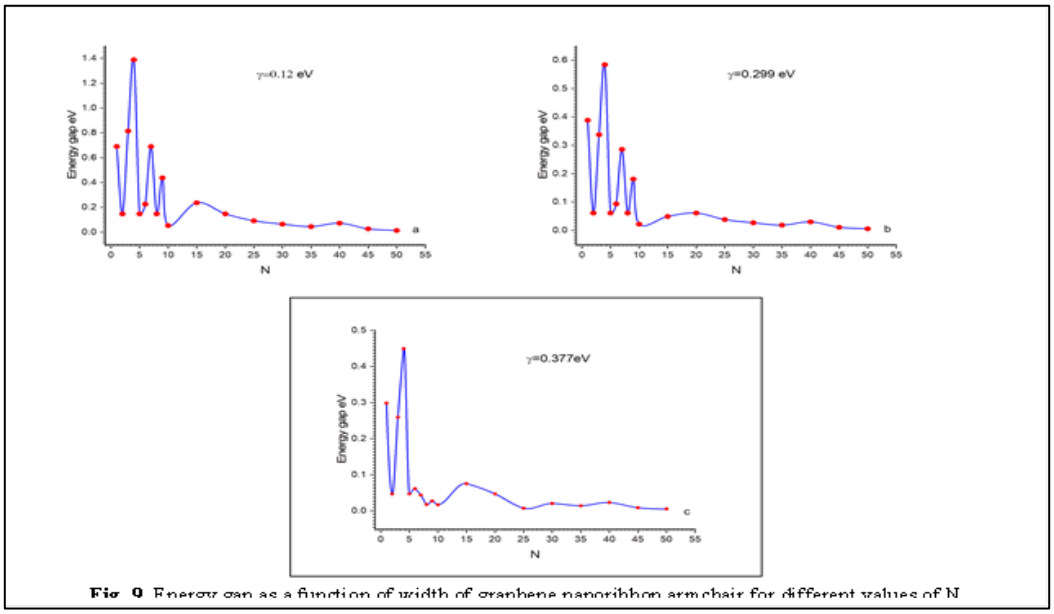

Fig. 9 Energy gap as a function of width of graphene nanoribbon armchair for different values of N

Fig. 9. Energy gap as a function of width of graphene nanoribbon armchair for different values of N

Publisher: SARC Publisher

All the data we obtained are in close proximity to the Fermi surface at the Dirac points in the first Berlon area. Upon revisiting Table 1, we observe an intriguing phenomenon: the energy gap values remain stable despite variations in the nanoribbon's width for N = 2, 5, 8, and 20. Specifically, this stability is evident for γ values of 0.12 and 0.29, while a delay in this stability occurs at N = 8 when $\gamma = 0.377$. It is important to observe that once N reaches certain values, the characteristics of graphene shift from those of a semiconductor with a suitable energy gap to those of a nearly conductive material. This transition has significant implications for the production of nanodevices. As the width of the nanoribbon increases, the energy gap decreases and the energy bands at the Dirac points start to flatten. It is worth noting that the flattening of the energy bands occurs more rapidly when $\gamma = 0.377$, indicating a higher electron hopping energy. Armchair graphene bands have a natural behaviour characterised by a mild edge effect, in contrast to zigzag bands, which have a large impact on the electrical characteristics. As the width increases, the nanoribbon approaches a state of

being a completely flat graphene sheet. Graphene is a well-known semiconductor that lacks an energy
gap, meaning it acts similarly to a metal. Additionally, the impact of transverse wave vector quantisation diminishes as the width of graphene grows. In this work, we observed that at N=25, the values of γ were 0.12 and 0.29, respectively. Additionally, at N=15, the value of γ was 0.377. This indicates that when the electron hopping energy and the width of the armchair graphene nanoribbon with AB stacking increase, the behaviour transitions from being a semiconductor to a conductor. Regarding the exceptional instance of the energy gap values described earlier, we were unable to provide a plausible physical explanation to account for this particular occurrence.

FINAL CONCLUSIONS

The present work investigated the electronic structure of a graphene nanoribbon by employing the AB technique. The study examined how the width of the nanoribbon and the energy of electron hopping between the bilayer affect its electronic structure. Based on the observed data, we have determined that there is a distinct correlation between the energy of electron hopping and the values of the energy gap. This connection is non-linear and inverse, meaning that as the energy of electron hopping decreases, the energy gap values increase. Regarding the width, we observed that decreasing the width resulted in bigger energy gap values. This is because the quantisation of the transverse wave vector has a substantial impact. As the width of the nanoribbon rose, the behaviour transitioned from being semiconductor-like to conductive. The most optimal outcomes for producing semiconductor materials using graphene, with an energy gap similar to traditional semiconductors, were seen when the values of N were 4, 3, 7, 9, and 15, and the hopping energy was nearly equivalent to $\gamma = 0.12$ and 0.29. Hence, this theoretical investigation can serve as a valuable addition to our understanding of the electronic characteristics of graphene under specific circumstances. Furthermore, it can aid in keeping up with the remarkable advancements in the production of nanodevices using graphene.

REFERENCES

1. Wasalathilake, K. C., Li, H., Xu, L., & Yan, C. "Recent advances in graphene based materials as anode materials in sodium-ion batteries." *Journal of Energy Chemistry* 42 (2020): 91-107.
2. Potbhare, A. K., Aziz, S. T., Ayyub, M. M., Kahate, A., Madankar, R., Wankar, S., ... & Chaudhary, R. G. "Bioinspired graphene-based metal oxide nanocomposites for photocatalytic and electrochemical performances: an updated review." *Nanoscale Advances* 6.10 (2024): 2539-2568.
3. Gosling, J. H., Makarovsky, O., Wang, F., Cottam, N. D., Greenaway, M. T., Patanè, A., ... & Fromhold, T. M. "Universal mobility characteristics of graphene originating from charge scattering by ionised impurities." *Communications Physics* 4.1 (2021): 30.
4. Gosling, J. H., Makarovsky, O., Wang, F., Cottam, N. D., Greenaway, M. T., Patanè, A., ... & Fromhold, T. M. "Universal mobility characteristics of graphene originating from charge scattering by ionised impurities." *Communications Physics* 4.1 (2021): 30.
5. Kotov, V. N., Uchoa, B., Pereira, V. M., Guinea, F., & Castro Neto, A. H. "Electron-electron interactions in graphene: Current status and perspectives." *Reviews of modern physics* 84.3 (2012): 1067-1125.
6. Di Bernardo, I., Avvisati, G., Chen, C., Avila, J., Asensio, M. C., Hu, K., ... & Betti, M. G. "Topology and doping effects in three-

Publisher: SARC Publisher

dimensional nanoporous graphene." *Carbon* 131 (2018): 258-265.
7. Gosling, J. H., Makarovsky, O., Wang, F., Cottam, N. D., Greenaway, M. T., Patanè, A., ... & Fromhold, T. M. "Universal mobility characteristics of graphene originating from charge scattering by ionised impurities." *Communications Physics* 4.1 (2021): 30.
8. Neto, C., Antonio H., et al. "The electronic properties of graphene." *Reviews of modern physics* 81.1 (2009): 109-162.
9. Barlocco, I., Capelli, S., Lu, X., Tumiati, S., Dimitratos, N., Roldan, A., & Villa, A. "Role of defects in carbon materials during metal-free formic acid dehydrogenation." *Nanoscale* 12.44 (2020): 22768-22777.
10. Novoselov, K. S., Morozov, S. V., Mohinddin, T. M. G., Ponomarenko, L. A., Elias, D. C., Yang, R., ... & Geim, A. K. "Electronic properties of graphene." *physica status solidi (b)* 244.11 (2007): 4106-4111.
11. Balandin, A. A. "Thermal properties of graphene and nanostructured carbon materials." *Nature materials* 10.8 (2011): 569-581.
12. Renteria, J. D., Nika, D. L., & Balandin, A. A. "Graphene thermal properties: applications in thermal management and energy storage." *Applied sciences* 4.4 (2014): 525-547.
13. Enoki, T., Fujii, S., & Takai, K. "Zigzag and armchair edges in graphene." *Carbon* 50.9 (2012): 3141-
14. Yang, G., Li, L., Lee, W. B., & Ng, M. C. "Structure of graphene and its disorders: a review." *Science and technology of advanced materials* 19.1 (2018): 613-648.
15. Zhan, D., Yan, J., Lai, L., Ni, Z., Liu, L., & Shen, Z. "Engineering the electronic structure of graphene." *Advanced Materials* 24.30 (2012): 4055-4069.
16. Wakabayashi, K., Sasaki, K. I., Nakanishi, T., & Enoki, T. "Electronic states of graphene nanoribbons and analytical solutions." *Science and technology of advanced materials* 11.5 (2010): 054504.
17. Liu, J., & Feng, X. "Synthetic Tailoring of graphene nanostructures with zigzag-edged topologies: progress and perspectives." *Angewandte Chemie International Edition* 59.52 (2020): 23386-23401.
18. Wakabayashi, K., Takane, Y., Yamamoto, M., & Sigrist, M. "Edge effect on electronic transport properties of graphene nanoribbons and presence of perfectly conducting channel." *Carbon* 47.1 (2009): 124-137.
19. Sun, Q., Gröning, O., Overbeck, J., Braun, O., Perrin, M. L., Borin Barin, G., ... & Ruffieux, P. "Massive Dirac fermion behavior in a low bandgap graphene nanoribbon near a topological phase boundary." *Advanced materials* 32.12 (2020): 1906054.
20. Majid, M. J., & Alaa, M. H. "Trembling motion of the wave packet in armchair graphene nanoribbons (AGNRs)." *International Journal of Modern Physics B* 32.32 (2018): 1850364.
21. Lavor, I. R., Da Costa, D. R., Chaves, A., Sena, S. H. R., Farias, G. A., Van Duppen, B., & Peeters, F. M. "Effect of zitterbewegung on the propagation of wave packets in ABC-stacked multilayer graphene: an analytical and computational approach." *Journal of Physics: Condensed Matter* 33.9 (2020): 095503.
22. Lee, J. H., Avsar, A., Jung, J., Tan, J. Y., Watanabe, K., Taniguchi, T., ... & Özyilmaz, B. "Van der Waals force: a dominant factor for reactivity of graphene." *Nano letters* 15.1 (2015): 319-325.
23. Richter, N., Chen, Z., Tries, A., Prechtl, T., Narita, A., Müllen, K., ... & Kläui, M. "Charge transport mechanism in networks of armchair graphene nanoribbons." *Scientific reports* 10.1 (2020): 1988.
24. Behura, S. K., Wang, C., Wen, Y., & Berry, V. "Graphene–semiconductor heterojunction sheds light on emerging photovoltaics." *Nature Photonics* 13.5 (2019): 312-318.
25. Zhang, J., Ragab, T., & Basaran, C. "Comparison of fracture behavior of defective armchair and zigzag graphene nanoribbons." *International Journal of Damage Mechanics* 28.3 (2019): 325-345.
26. Kim, J., Lee, N., Min, Y. H., Noh, S., Kim, N. K., Jung, S., ... & Yamada, Y. "Distinguishing zigzag and armchair edges on graphene nanoribbons by X-ray photoelectron and Raman spectroscopies." *ACS omega* 3.12 (2018): 17789-17796.
27. Thomson, A., Chatterjee, S., Sachdev, S., & Scheurer, M. S. "Triangular antiferromagnetism on the honeycomb lattice of twisted bilayer graphene." *Physical Review B* 98.7 (2018): 075109.

Publisher: SARC Publisher

28. Molitor, F., Güttinger, J., Stampfer, C., Dröscher, S., Jacobsen, A., Ihn, T., & Ensslin, K. "Electronic properties of graphene nanostructures." *Journal of Physics: Condensed Matter* 23.24 (2011): 243201.
29. Ren, W., Chen, W., Liu, X., & Zhang, X. "Strain induced magnetic phase transition in slightly doped graphene nanoribbons." *Physics Letters A* 426 (2022): 127886.
30. Tene, T., Guevara, M., Viteri, E., Maldonado, A., Pisarra, M., Sindona, A., ... & Bellucci, S. "Calibration of fermi velocity to explore the plasmonic character of graphene nanoribbon arrays by a semi-analytical model." *Nanomaterials* 12.12 (2022): 2028.
31. Partoens, B., & Peeters, F. M. "From graphene to graphite: Electronic structure around the K point." *Physical Review B—Condensed Matter and Materials Physics* 74.7 (2006): 075404.
32. Chung, D. D. L. "Review graphite." *Journal of materials science* 37.8 (2002): 1475-1489.
33. Konschuh, S., Gmitra, M., Kochan, D., & Fabian, J. "Theory of spin-orbit coupling in bilayer graphene." *Physical Review B—Condensed Matter and Materials Physics* 85.11 (2012): 115423.
34. Herman, F. "The electronic energy band structure of silicon and germanium." *Proceedings of the IRE* 43.12 (2007): 1703-1732.
35. Gayen, R. N., Hussain, S., Bhar, R., & Pal, A. K. "Synthesis and characterization of indium phosphide films prepared by co-evaporation technique." *Vacuum* 86.9 (2012): 1240-1247.

Source of support: Nil; **Conflict of interest:** Nil.

Cite this article as:
Bashar, H. Z. " Effect of Jumping Energy Coefficient on Armchair-Type Graphene Energy Gap." *Sarcouncil Journal of Applied Sciences* 5.9 (2025): pp 32-42.

Publisher: SARC Publisher